Supporting Information

Approaching the Minimum Lattice Thermal Conductivity in TiCoSb Half-Heusler Alloys by Intensified Point-Defect Phonon Scattering

Ajay Kumar Verma[1, 2, 3, 4], Shamma Jain[1, 2], Kishor Kumar Johari[1, 2], Christophe Candolfi[5], Bertrand Lenoir[5, *], Sumeet Walia[3, 4], S. R. Dhakate[1, 2], and Bhasker Gahtori[1, 2, *]

[1]*CSIR-National Physical Laboratory, Dr. K.S. Krishnan Marg, New Delhi 110012, India*
[2]*Academy of Scientific & Innovative Research (AcSIR), Ghaziabad, 201002, India*
[3]*Functional Materials and Microsystems Research Group and the Micro Nano Research Facility, RMIT University, Melbourne, VIC 3001, Australia*
[4]*School of Engineering, RMIT University, GPO Box 2476, Melbourne, Victoria 3001, Australia*
[5]*Institut Jean Lamour UMR 7198 CNRS – Université de Lorraine Campus ARTEM, 2 allée André Guinier, BP 50840, Nancy 54011, France*

Calculated room-temperature density-of-states effective mass:

To understand the electronic transport behavior, density-of-states effective mass ($m_{DOS}{}^{*}$) was calculated at room temperature using the following equation [1]:

$$m_{DOS}{}^{*} \approx \frac{h^2}{2k_BT}\left\{\frac{3p_H}{16\sqrt{\pi}}\left[exp\left(\frac{|\alpha|}{k_B/e}-2\right)-0.17\right]\right\}^{2/3} \quad \text{(S-1)}$$

Here, *e* represents electronic charge, *h* is Planck's constant, and k_B is Boltzmann constant. Fig. S3 shows that the substituting Fe and Sn for Co and Sb, respectively, increases $m_{DOS}{}^{*}$, which is due to the effect of valence band convergence [2, 3]. These results further suggest that heavy alloying of Zr and Hf on the Ti site and the small concentration of Bi on the Sb site may lower the effect of band convergence.

The minimum limit of lattice thermal conductivity for TiCoSb:

*Corresponding authors: bhasker@nplindia.org, bertrand.lenoir@univ-lorraine.fr
Tel.: +91-11-45608556; Fax: +91-11-45609310

The minimum lattice thermal conductivity of TiCoSb at RT has been calculated using the model developed by Cahill and Pohl [4]:

$$\kappa_{L,min} = \left(\frac{\pi}{6}\right)^{1/3} k_B N^{2/3} \sum_i v_i \left(\frac{T}{\theta_i}\right)^2 \int_0^{\theta_i/T} \frac{x^3 e^x}{(e^x-1)^2} dx \quad \text{(S-2)}$$

The sum is taken over two transverse modes and one longitudinal mode with their corresponding sound velocities v_i, N is the density of atoms and θ_i is the cut off frequency of polarization calculated by $\theta_i = v_i(\hbar/k_B)(6\pi^2 N)^{1/3}$. Here, the longitudinal and transverse sound velocities (v_L= 5699 m s^{-1} and v_T = 3237 m s^{-1}, respectively) of TiCoSb were taken from the literature [5].

Calculations of relaxation time of different scattering mechanisms:

The relaxation time expression of point defect scattering, which originates from mass and strain field fluctuations in the lattice can be expressed as[6]:

$$\tau_{PD}^{-1} = \frac{V\omega^4}{4\pi v^3} \Gamma = \frac{V\omega^4}{4\pi v^3} (\Gamma_M + \Gamma_S) \quad \text{(S-3)}$$

where V is the volume per atom, $\Gamma = \Gamma_M + \Gamma_S$ is the total disorder scattering parameter with Γ_M and Γ_S the disorder scattering parameters owing to the difference in mass and strain field, respectively. Γ can be estimated from the κ_L data according to the equations[7]:

$$\frac{\kappa_L^d}{\kappa_L^o} = \frac{tan^{-1}(u)}{u}$$

$$u^2 = \frac{\pi^2 \theta_D V}{h v^2} \kappa_L^o \Gamma_{exp} \quad \text{(S-4)}$$

where κ_L^o represents the lattice thermal conductivity of the ordered system and κ_L^d is the lattice thermal conductivity of the alloyed compound. In the present study, we assumed that $TiCo_{0.85}Fe_{0.15}Sb$ sample is ordered, while the Zr, Hf and Bi-substituted samples were considered as disordered. To calculate the disorder scattering parameters, we assumed $\Gamma =$

Γ_{exp}. The chemical compositions of the samples can be conveyed as $A_{1g_1}A_{2g_2}A_{3g_3}A_{4g_4}\ldots A_{ng_n}$, A_i (i=1, 2, 3, 4,..n) is the crystallographic sublattice, and g_i is the respective degeneracy. The different type of atoms can occupy these sublattices, so that the mass, radius, and fractional occupancy can be expressed as M_i^k, r_i^k, and f_i^k due to the k^{th} atom at the i^{th} sublattice. For the series $Ti_{0.5}Zr_{0.2}Hf_{0.3}Co_{0.85}Fe_{0.15}Sb_{1-x}Bi_x$, i=1, 2, and 3 for the Ti, Co, and Sb sublattice, respectively, with the corresponding degeneracies $g_1 = g_2 = g_3 = 1$. The scattering parameters due to mass and strain field fluctuations can be calculated as[7]:

$$\Gamma_M = \frac{\sum_{i=1}^{3} g_i\left(\frac{\bar{M}_i}{\bar{\bar{M}}}\right)^2 f_i^1 f_i^2\left(\frac{M_i^1 - M_i^2}{\bar{M}_i}\right)^2}{\sum_{i=1}^{3} g_i} \quad \text{(S-5)}$$

and

$$\Gamma_S = \frac{\sum_{i=1}^{3} g_i\left(\frac{\bar{M}_i}{\bar{\bar{M}}}\right)^2 f_i^1 f_i^2\left(\frac{r_i^1 - r_i^2}{\bar{r}_i}\right)^2}{\sum_{i=1}^{3} g_i}\varepsilon_i \quad \text{(S-6)}$$

In Eq. S-3 and S-4, $\bar{M}_i = \sum_k f_i^k M_i^1$ is the average atomic mass at the i^{th} sublattice, $\bar{r}_i = \sum_k f_i^k r_i^1$ is the average atomic radius of the i^{th} sublattice, $\bar{\bar{M}} = \sum_{i=1}^{3} g_i \bar{M}_i / \sum_{i=1}^{3} g_i$ is the average atomic mass of the compound, and ε_i is the phenomenological adjustable parameters for the i^{th} sublattice.

The thermodynamic average Grüneisen parameter (γ), which characterizes the lattice anharmonicity, can be calculated from ε_i using the following equation [8, 9]:

$$\varepsilon_i = \frac{2}{9}\left[\frac{6.4(1+\nu_P)}{(1-\nu_P)}\gamma\right]^2 \quad \text{(S-7)}$$

where ν_P is the Poisson ratio that can be obtained from the relation [10]:

$$\nu_P = \frac{1-2\left(\nu_T/\nu_L\right)^2}{2-2\left(\nu_T/\nu_L\right)^2} \quad \text{(S-8)}$$

The Grüneisen parameter for undoped sample $TiCo_{0.85}Fe_{0.15}Sb$ was assessed using the equation $\gamma = 3(1+\nu_P)/2(2-3\nu_P)$ [10].

Umklapp phonon scattering effectively reduces the lattice thermal conductivity for T > $0.1\theta_D$ [11]. The relaxation time for Umklapp phonon scattering can be determined by [6]:

$$\tau_U^{-1} = \frac{\hbar\gamma^2}{Mv^2\theta_D}\omega^2 T e^{(-\theta_D/3T)} \quad \text{(S-9)}$$

where, M is the average molar mass of atoms, γ is the above-mentioned Grüneisen parameter. In polycrystalline samples, grain boundary scattering is also at play and can be determined by the simple equation $\tau_B^{-1} = v/L_G$ [12], where L_G is the grain size. Here, L_G was estimated by the Williamson-Hall method using the PXRD data.

Calculation $(ZT)_{Eng}$:

The cumulative temperature dependency (CTD) model was taken into account in order to determine the energy conversion efficiency based on the temperature dependence of TE transport characteristics and the *ZT* values of all samples. For devices operating under a large temperature difference, the engineering dimensionless thermoelectric figure of merit $(ZT)_{Eng}$ determines the maximum conversion efficiency by taking into account the temperature dependence of α, ρ, and κ according to the following relations [13, 14]

$$(ZT)_{Eng} = \frac{\left(\int_{T_c}^{T_h}\alpha(T)dT\right)^2}{\int_{T_c}^{T_h}\rho(T)dT\int_{T_c}^{T_h}\kappa(T)dT}\Delta T \quad (10)$$

where T_h is the hot side temperature, T_c is the cold side temperature, ΔT is the temperature difference between the hot and cold sides, and ρ is the electrical resistivity. For all the calculations, we assumed a fixed T_c of 323 K.

Tables

Table S-1: Rietveld refinement parameters of all the samples $Ti_{0.5}Zr_{0.2}Hf_{0.3}Co_{0.85}Fe_{0.15}Sb_{1-x}Bi_x$.

Sample Details	$\mathbf{R_p}$	$\mathbf{R_{wp}}$	$\mathbf{R_e}$	χ^2	***a* (Å)**
***x* = 0**	40.4	27.1	12.9	4.399	5.9682
***x* = 0.01**	24.4	18.2	9.3	3.827	5.9692
***x* = 0.02**	27.4	20.9	10.6	3.912	5.9689
***x* = 0.03**	24.6	18.5	9.83	3.557	5.9678
***x* = 0.04**	27.6	21.3	10.6	4.076	5.9773

Figures

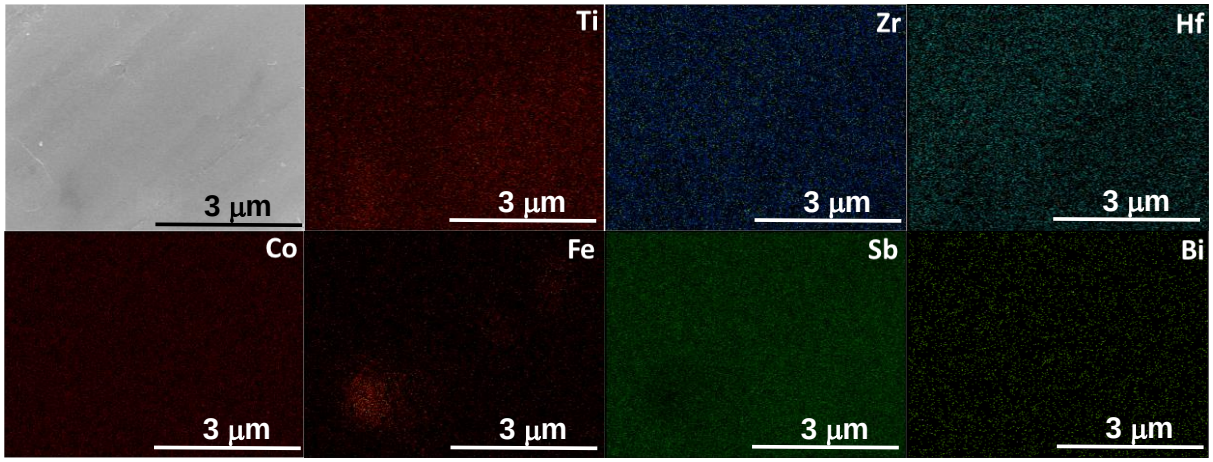

Fig. S-1: Elemental mapping of the sample $Ti_{0.8}Zr_{0.2}Hf_{0.3}Co_{0.85}Fe_{0.15}Sb_{0.96}Bi_{0.04}$.

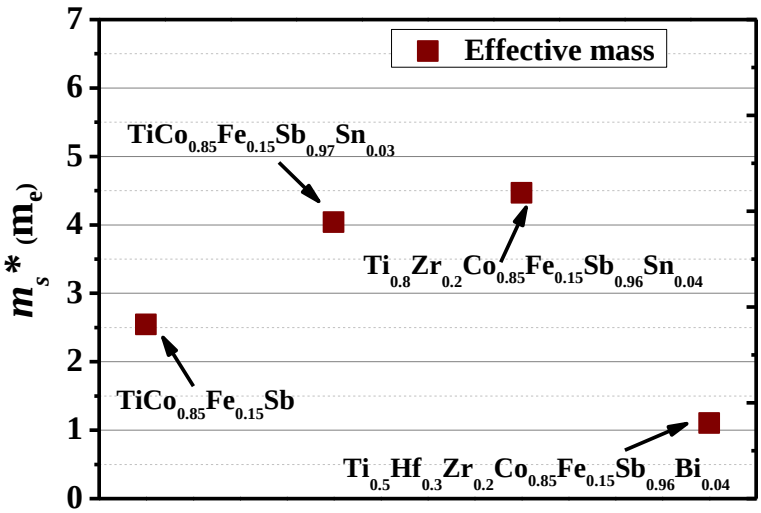

Fig. S-2: Comparision of density-of-states effective masses calculated at room temperature with those previously reported for $TiCo_{0.85}Fe_{0.15}Sb$, $TiCo_{0.85}Fe_{0.15}Sb_{0.97}Sn_{0.03}$ [2] and $Ti_{0.8}Zr_{0.2}Co_{0.85}Fe_{0.15}Sb_{0.96}Sn_{0.04}$ [3].

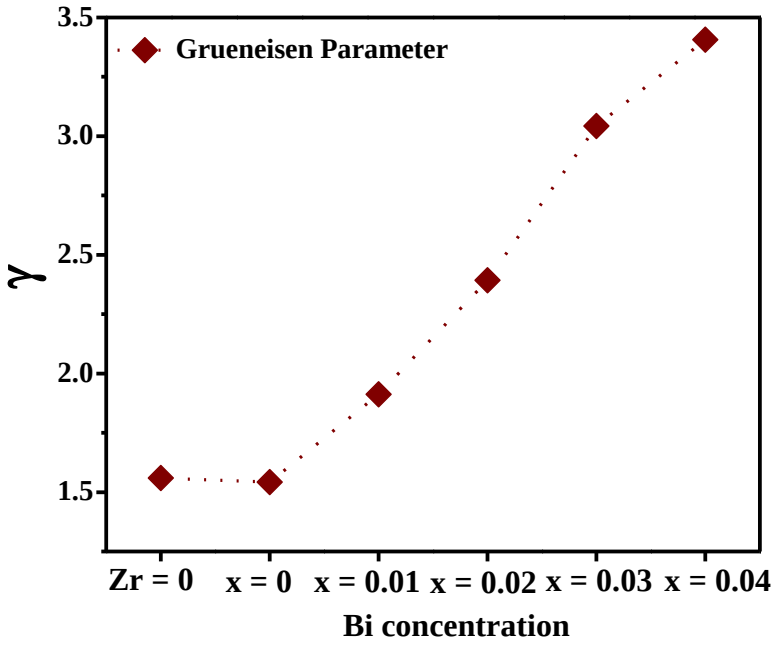

Fig. S-3: Grüneisen parameter γ of the samples $Ti_{0.5}Zr_{0.2}Hf_{0.3}Co_{0.85}Fe_{0.15}Sb_{1-x}Bi_x$ at 450 K.

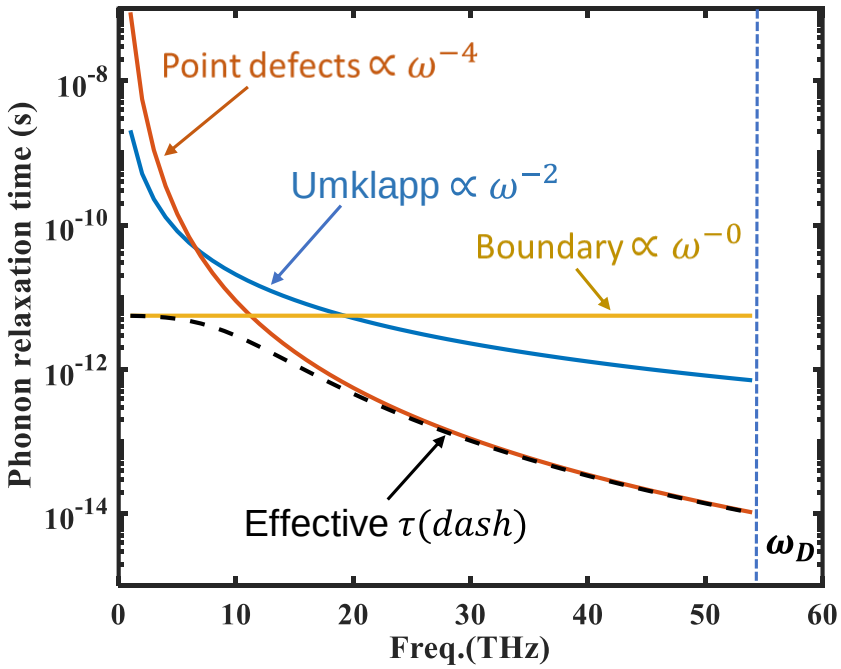

Fig. S-4: The calculated phonon relaxation time for the sample $Ti_{0.8}Zr_{0.2}Hf_{0.3}Co_{0.85}Fe_{0.15}Sb_{0.96}Bi_{0.04}$.

References:

1. Zevalkink, A., et al., *A practical field guide to thermoelectrics: Fundamentals, synthesis, and characterization.* Applied Physics Reviews, 2018. **5**(2): p. 021303.
2. Verma, A.K., et al., *Realization of Band Convergence in p-Type TiCoSb Half-Heusler Alloys Significantly Enhances the Thermoelectric Performance.* ACS Applied Materials & Interfaces, 2023. **15**(1): p. 942-952.
3. Verma, A.K., et al., *Coupling of electronic transport and defect engineering substantially enhances the thermoelectric performance of p-type TiCoSb HH alloy.* Journal of Alloys and Compounds, 2023. **947**: p. 169416.
4. Cahill, D.G., S.K. Watson, and R.O. Pohl, *Lower limit to the thermal conductivity of disordered crystals.* Physical Review B, 1992. **46**(10): p. 6131.
5. Sekimoto, T., et al. *Thermoelectric and thermophysical properties of TiCoSb, ZrCoSb, HfCoSb prepared by SPS*. in *ICT 2005. 24th International Conference on Thermoelectrics, 2005.* 2005. IEEE.
6. Xie, H., et al., *Beneficial contribution of alloy disorder to electron and phonon transport in half‐heusler thermoelectric materials.* Advanced Functional Materials, 2013. **23**(41): p. 5123-5130.
7. Yang, J., G. Meisner, and L. Chen, *Strain field fluctuation effects on lattice thermal conductivity of ZrNiSn-based thermoelectric compounds.* Applied physics letters, 2004. **85**(7): p. 1140-1142.
8. Wan, C., et al., *Effect of point defects on the thermal transport properties of (La x Gd 1− x) 2 Zr 2 O 7: Experiment and theoretical model.* Physical Review B, 2006. **74**(14): p. 144109.
9. Liu, Y., et al., *Demonstration of a phonon-glass electron-crystal strategy in (Hf, Zr) NiSn half-Heusler thermoelectric materials by alloying.* Journal of Materials Chemistry A, 2015. **3**(45): p. 22716-22722.
10. Pei, Y.-L., et al., *High thermoelectric performance of oxyselenides: intrinsically low thermal conductivity of Ca-doped BiCuSeO.* NPG Asia Materials, 2013. **5**(5): p. e47-e47.
11. Slack, G.A. and S. Galginaitis, *Thermal conductivity and phonon scattering by magnetic impurities in CdTe.* Physical Review, 1964. **133**(1A): p. A253.
12. Goldsmid, H. and A. Penn, *Boundary scattering of phonons in solid solutions.* Physics Letters A, 1968. **27**(8): p. 523-524.
13. Kim, H.S., et al., *Relationship between thermoelectric figure of merit and energy conversion efficiency.* Proceedings of the National Academy of Sciences, 2015. **112**(27): p. 8205-8210.
14. Kim, H.S., W. Liu, and Z. Ren, *The bridge between the materials and devices of thermoelectric power generators.* Energy & Environmental Science, 2017. **10**(1): p. 69-85.